2021 43rd Annual International Conference of the
IEEE Engineering in Medicine & Biology Society (EMBC)
Oct 31 - Nov 4, 2021. Virtual Conference

A Low-rank Spatiotemporal based EEG Multi-Artifacts Cancellation Method for Enhanced ConvNet-DL's Motor Imagery Characterization

Oluwarotimi Williams Samuel*, Mojisola Grace Asogbon, Esugbe Ejay, Yanjuan Geng, Alberto López-Delis, Yazan Ali Jarrah, Oluwagbenga Paul Idowu, Shixiong Chen, Peng Fang, and Guanglin Li*, *IEEE Senior Member*

***Abstract*— Multi-channel Electroencephalograph (EEG) signal is an important source of neural information for motor imagery (MI) limb movement intent decoding. The decoded MI movement intent often serve as potential control input for brain-computer interface (BCI) based rehabilitation robots. However, the presence of multiple dynamic artifacts in EEG signal leads to serious processing challenge that affects the BCI system in practical settings. Hence, this study propose a hybrid approach based on Low-rank spatiotemporal filtering technique for concurrent elimination of multiple EEG artifacts. Afterwards, a convolutional neural network based deep learning model (ConvNet-DL) that extracts neural information from the cleaned EEG signal for MI tasks decoding was built. The proposed method was studied in comparison with existing artifact removal methods using EEG signals of transhumeral amputees who performed five different MI tasks. Remarkably, the proposed method led to significant improvements in MI task decoding accuracy for the ConvNet-DL model in the range of 8.00~13.98%, while up to 14.38% increment was recorded in terms of the MCC: Mathew correlation coefficients at p<0.05. Also, a *signal to error ratio* of more than 11 dB was recorded by the proposed method.**

***Clinical Relevance*— This study showed that a combination of the proposed hybrid EEG artifact removal method and ConvNet-DL can significantly improve the decoding accuracy of MI upper limb movement tasks. Our findings may provide potential control input for BCI rehabilitation robotic systems.**

I. INTRODUCTION

The continuous rise in number of persons with upper limb motor function loss due to amputation or neurological dysfunction (Stroke) has necessitated the need to develop a rehabilitation device. For upper limb amputees, assistive devices driven by surface myoelectric pattern recognition (PR) have been explored as a possible way to restore their lost limb functions [1-2]. The wide interest in PR based control strategies is partially due to their non-invasiveness and capability to offer intuitive control for multiple degrees of freedom function in a physiologically appropriate manner [3-5]. In myoelectric PR based prosthesis, it is required that repeatable muscle activation patterns for specific limb movement task can be produced, from which the corresponding motion intent can be decoded to provide control input to the device [5]. However, insufficient muscle sites for acquisition of motor control information especially in persons with high-level amputation has affected the deployment of such a control scheme in practical settings. The above challenge has prompted researchers to explore electroencephalograph (EEG) signals, as an alternative source of neural control information in the recent years [6]. Moreover, EEG is non-invasive, has excellent temporal resolution, and can be easily recorded [6-7]. Considering these merits, motor imagery (MI) decoding from EEG signals are currently being explored as potential control input for BCI driven rehabilitation robots [2]. However, confounding factors including non-physiological and physiological artifacts hinders adequate processing of EEG signals, which affects decoding of inherent MI tasks [7-8]. With the aid of a simple filter design and proper experimental protocol, artifacts from non-physiological sources can be greatly attenuated [9]. On the other hand, physiologically triggered artifacts are difficult to remove, and habitually require the adoption of dedicated algorithms [9-10].

Attempts have been made to resolve the impact of physiologically triggered EEG artifacts using automated and semi-automated methods that employ either regression or blind source separation approaches [7, 11-14]. That is, time-space based principal component analysis and regression techniques have been used to cancel ocular artifacts from multi-channel EEG recordings [11-14]. Similarly, methods based on independent component and canonical correlation analyses have been applied to attenuate eye blink, movement-related, and muscle artifacts from EEG signals [7, 11-12]. Moreover, hybrid approaches, multi artifact rejection algorithms and statistical thresholding methods have been proposed in the recent years [13]. Though these methods have shown good performances, they mainly focus on isolating single artifact per time from an ensemble of signals and require calibration and/or reference electrode, leading to increased complexity of their application in practical settings. Thus, the limitation of the existing methods and their non-exploration in the space of MI-EEG recordings for multiple artifacts removal from a single EEG trial may be a major inhibitor to their clinical application in BCI systems. Additionally, extracting relevant features from the underlying signal of interest (clean EEG signal) constitute an essential aspect of the entire pattern recognition based BCI control scheme [14]. Hence, the adoption of convolutional neural network based deep learning model (ConvNet-DL) for automatic extraction of spatial and temporal descriptors that correlates well with the neural information inherent in the clean EEG signal may enhance the overall system performance [14].

In this study, a ConvNet-DL model that integrates eigenvalue decomposition (EVD) with low rank spatio-temporal filtering (STF) technique for concurrent removal of multiple artifacts from EEG signal is implemented, for robust

The research work was supported in part by the National Natural Science Foundation of China under grants (#82050410452, #U1613222, #61771462, #61773364), Shenzhen Science and Technology Program (#SGLH20180625142402055), Shenzhen Governmental Basic Research Grant (#JCYJ20180507182241622), and National Key Research & Development Program of China (2017YFA0701103).

O.W. Samuel, M.G. Asogbon, Y.A. Jarrah, O.P. Idowu, Y. Geng, S. Chen, P. Fang, and G. Li are with the CAS Key Laboratory of Human-Machine Intelligence-Synergy Systems, Shenzhen Institute of Advanced Technology (SIAT), Chinese Academy of Sciences (CAS), Shenzhen, Guangdong 518055, China (Correspondence: e-mail: samuel@siat.ac.cn and gl.li@siat.ac.cn).

M.G. Asogbon, Y.A. Jarrah, and O.P. Idowu are also with the Shenzhen College of Advanced Technology, University of Chinese Academy of Sciences, Shenzhen, Guangdong 518055, China.

E. Nsugbe is an Independent Researcher in the U.K.

A. Alberto López-Delis is with the Center of Medical Biophysics, University of Oriente, Cuba.

and accurate MI task decoding. Specifically, based on the learned statistical properties of the EEG signal, the method attempt to isolate multiple artifact without any requirement for calibration/reference channel. The proposed method performance was evaluated using EEG recordings of transhumeral amputees and then compared with notable existing artifact removal methods.

II. METHODS

A. Participants information

In this study, four male transhumeral amputee subjects with average residual limb of length 25.50 ± 4.50 cm were recruited [2].The experimental procedures were clearly described to them, and they agreed to take part in the study and signed the consent form. In addition, they agreed that their data can be used for publication purpose to promote scientific research. The experimental protocol was approved by the Institutional Review Board of Shenzhen Institutes of Advanced Technology, Chinese Academy of Sciences with a reference identification number of *SIAT-IRB-150515-H0077*.

B. Data collection and preprocessing

For the EEG signal recording, a 64-channel Al-AgCl recording system (EasyCap, Herrsching, Germany) was utilized following the international 10-20 electrode placement standard (Fig. 1). Each subject was instructed to imagine performing five distinctive limb movement tasks (denoted as MI tasks) whose images appear randomly on a computer screen. To avoid mental fatigue, a rest image display between two consecutive MI tasks. Precisely, the MI tasks (which comprised of hand close: HC, hand open: HO, wrist pronation: WP, wrist supination: WS and no movement: NM) were observed for 5s with a 5s rest between consecutive tasks.

Fig. 1. Placement of Multi-channel EEG electrodes on the arm of a representative subject.

Meanwhile, the signals were recorded with a sampling rate of 1000 Hz and the EEGLAB toolbox (version 13.4.4b) was used to visualize and select the electrode channels located around the motor cortex region for extraction of epochs corresponding to the various MI tasks. Further preprocessing and implementation was carried out using TensorFlow in JetBrains PyCharm Professional (2020.1 Edition).

C. Proposed Multi Artifacts Removal Algorithm

Suppose the MI-EEG signal, $z[t] \in P^M$ at a sampling time (t) is given as in equation (1):

$$z[t] = x[t] + y[t] \tag{1}$$

where $x[t] \in P^M$ is a vector P of dimension M that contains the original neural signals and $y[t]$ denotes different types of artifacts contained in the original neural signals. Then, the mean subtraction technique is firstly applied after which the covariance matrices of the signals denoted as P_{zz}, P_{xx} and P_{yy}, are determined, respectively. With the assumption that x and y are not correlated, then a relationship is formulated as in (2):

$$P_{zz} = P_{xx} + P_{yy} \tag{2}$$

It is worth noting that the proposed method is modelled based on some presumptions: the noise is an additive component of the signal; the real neural signal and artifact-contaminated signal are uncorrelated. These are premise that need to be met in the modeling of EEG signals.

Linearly combining the channels in z, the STF based on Wiener filter generates an estimate ($\hat{y}$) of the multi-channel artifact signals y, that is $\hat{y} = W^T z$ where W is the linear estimator and superscript ^{T} is the conjugate transpose operator. The linear combination is then optimized using the *mean square error* criterion in (3).

$$W^T = \underset{W}{\arg min} E\{\|y - W^T z\|^2\} \tag{3}$$

Practically, the signal correlation matrix P_{zz} is often not available, but it can be estimated using a sample averaging technique. Thus, the $M \times N$ observation matrix Z can be defined, where the n^{th} column corresponds to an observation of Z at a particular time. Using an artifact detection approach, the N observations of Z can be separated into mutually exclusive sets, Z_a and Z_b, where the first contains N_a artifact contaminated samples while the second contains N_b artifact-free samples. This process allows P_{zz} to be estimated as in (4) while the artifact-free sample is estimated as in (5):

$$\hat{P}_{zz} = \frac{1}{N_a} Z_a Z_a^N \tag{4}$$

$$\hat{P}_{xx} = \frac{1}{N_b} Z_b Z_b^N \tag{5}$$

Meanwhile, by subtracting the estimated artifacts using the additive model of equation (1), the artifact-free MI-EEG neural signal is obtained via equation (6).

$$\hat{x} = z - \widehat{W}^N z \tag{6}$$

Thus, the mean subtraction process forces $\hat{P}_{yy}$ to be positive semi-definite thereby enhancing the estimation performance of the STF, especially in low SNR conditions in synergy with the eigenvalue decomposition outcomes [15].

D. ConvNet-DL Framework for MI-EEG task decoding

After eliminating multiple artifacts from the signals as described above, a ConvNet-DL model that extracts spatiotemporal features is built to decode the inherent MI tasks. The ConvNet-DL model mainly assigns learnable weights and biases during the feature extraction process to identify the MI tasks. The model's components includes convolutional layers: CLs, pooling layers: PLs and dense layers: DLs, as follows.

Suppose that the preprocessed signals is a two-dimensional vector expressed as in eqn. (7):

$$y = \begin{pmatrix} y_{11} & y_{12} & \cdots & y_{1j} \\ y_{21} & y_{22} & \cdots & y_{2j} \\ \cdots & \cdots & \cdots & \cdots \\ y_{k1} & y_{k2} & \cdots & y_{kj} \end{pmatrix} \tag{7}$$

where $k \times j$is the shape of the input vector y in the CLs, and convolution filter, W_i is applied to the input vector in eqn. (8).

$$W_i = \begin{pmatrix} W_{11} \\ W_{21} \\ \dots \\ W_{r1} \end{pmatrix} \tag{8}$$

where r is the length of W_i and $r < k$ in eqn. (8). The ConvNet-DL consist of two CLs while in each layer, a set of computations is performed to produce 32 and 64 output feature maps, respectively. Also, a ReLU activation function was applied to each output feature map to introduce nonlinearities into the ConvNet-DL model as shown in (9).

$$f(\alpha) = f(\, W_i \, \times y \, \times \, b_i) \tag{9}$$

where $W_i \in M^r$ is the weight matrix, b_i is the bias, f is the ReLU activation function, i is the filter index, for $i = 1,2.3, \dots, n$ and n is the number of filtering in the convolutional layers.

At the PLs, the dimension of the feature maps is reduced in order to decrease the processing time by down sampling it using a max-pooling function. After the last pooling layer, the output is flattened into a column vector and then fed into network. In this layer, classification is performed on the output via a softmax activation function to obtain the probabilities of the input belonging to a particular MI class while Adam optimizer and cross-entropy loss function were used to train the model. A dropout regularization technique was applied to avoid overfitting and the parameters were updated using back-propagation algorithm.

E. Data Analysis and Performance Evaluation

In this section, the performance of the proposed method was evaluated and compared with the existing preprocessing methods while the built ConvNet-DL model and a representative machine learning algorithm (linear discriminant analysis; LDA classifier) were used for the MI task decoding. The LDA model was used as benchmark due to its simple structure, low computational cost, and relatively good performance [16-18]. The evaluation was performed using *classification accuracy* (AC) and *Matthew correlation coefficient* (MCC), metrics, expressed in (10) and (11).

$$CA = \frac{Number\ of\ correctly\ classified\ samples}{Total\ number\ of\ testing\ samples} * 100\% \tag{10}$$

$$MCC = \frac{(TP * TN) - (FP * FN)}{\sqrt{(TP + FP)(TP + FN)(TN + FP)(TN + FN)}} \tag{11}$$

where TP: true positives, TN: true negatives, FP: false positives, and FN: false negatives as obtained from a confusion matrix. Also, the signal quality after artifact removal was studied using *signal to error ratio* (SER), shown in eqn. 12. The SER is computed over the artifact free-segments expressed in dB.

$$SER = \sum_{i=1}^{M} p_i \cdot \left(10 log_{10} \left(\frac{E\{(y_i)^2\}}{E\{(\hat{d}_i)^2\}} |_{CS} \right) \right) \tag{12}$$

where P_i is the normalized weights proportional to the artifact power per channel, y_i is the original signal, $\hat{d}_i$ is the artifact estimate, CS is the clean segment and AS is the artifact segment. Lastly, the statistical significance of our results was verified using paired sample t-test with a confidence, p<0.05.

III. Results

A. Analysis of the proposed method's performance in comparison to existing methods

The MI-EEG was preprocessed via the proposed method (STF-EVD) and the popular existing methods (ICA-INFOMAX and STF). Thereafter, the artifact-free signals were used to build a ConvNet-DL model that extracted spatiotemporal neural information for MI task decoding. Similarly, the feature sets described in [16-17] were extracted and used to build LDA-ML model for the MI task decoding, and the obtained results are presented in Fig. 2.

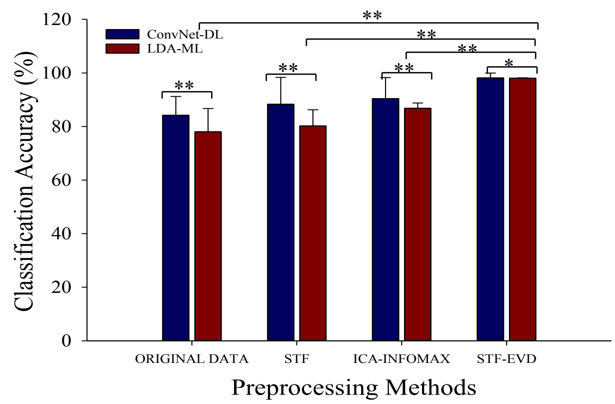

Fig. 2. Average decoding accuracy of the STF-EVD and existing methods across subjects & MI tasks with ConvNet-DL and LDA-ML.

From the results shown in Fig. 2, it can be seen that the proposed multi-artifact removal method led to consistently high decoding results for both the DL and ML models, achieving over 99.53% accuracy MI tasks and across subjects. Also, significant difference (p>0.05) was observed between the decoding results obtained when the original data that contained artifacts was used for the MI task decoding in comparison to the cleaned signals.

In the second phase of the evaluation, we further studied the performance of the EEG preprocessing methods using the MCC metric for the ConvNet-DL and LDA-ML models, as shown in Table 1.

Table 1: Average MCC values of the proposed and conventional EEG methods across subjects and MI tasks for ConvNet-DL and LDA-ML models.

	Original Data	*STF*	*ICA-INFOMAX*	*GEVD-MWF*
ConvNet-DL	0.8515	0.9511	0.9151	0.9953
LDA-ML	0.7449	0.7735	0.8515	0.9522

These results again revealed a performance trend consistent with the analyses in Fig. 2, where the proposed method achieved the highest MCC values for both the ConvNet-DL (0.9953) and LDA-ML (0.9522) models across MI tasks and subjects. This possibly prove the capability of proposed method in the reconstruction of clean neural signals for accurate and stable MI tasks decoding.

B. *Decoding individual MI task using the proposed method*

In this analysis, the possibility of decoding individual class of MI task after applying the proposed method for both the ConvNet-DL and LDA-ML models were examined as shown in Figure 3a and 3b, respectively. For the ConvNet-DL, accuracies of 100% were achieved for WS and NM, as against 99.56% and 95.69% for the LDA-ML. For both models, the least accuracy was around 95.00% as seen in Fig. 3, which seems good enough to yield adequate control input for practical BCI systems.

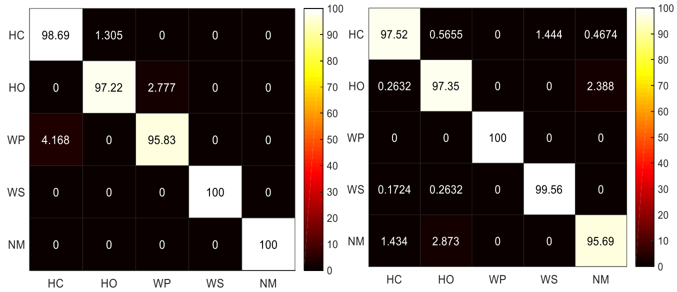

Fig. 3. Decoding of Individual MI task across subjects after applying the proposed method with (a) ConvNet-DL; (b) LDA-ML models.

C. Analysis of the quality of artifact removal by the proposed method.

Furthermore, the capability of the proposed method in isolating multiple artifacts from the signals across different time-delay parameter (0-5), was investigated based on the distortion level of the clean signal using SER metric (Fig. 4). The results are shown using a group-level boxplots while the dashed lines denote the performance measure trends for individual subjects (Fig. 4). It can be seen that the SER increases with the time delays employed in constructing the WF component of the proposed method, which helps separates artifacts from the neural signal of interest from the recordings. Interestingly, the increase was observed to be relatively larger at the first few delays (0-2) and became steady again at 3, after which it steadily rises, achieving over 11 SER (dB). This suggest that the proposed method's capability in eliminating artifacts increases corresponding with the increase in the time-delay parameter.

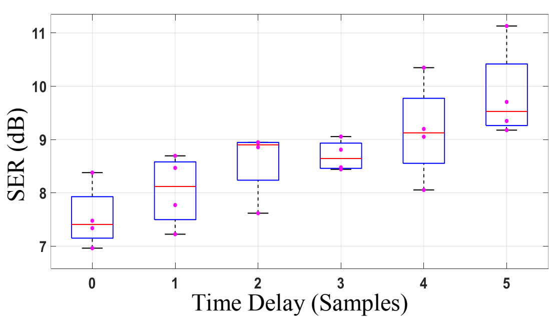

Fig. 4. Analysis of the signal to error ratio of the proposed method.

IV. Discussion and Conclusion

This study proposed a multi-artifact removal method that integrates eigenvalue decomposition and spatio-temporal filter techniques (STF-EVD), and further built a convolutional neural network based deep learning model (ConvNet-DL) to decode multiple classes of MI tasks using the cleaned signals.

To validate the effectiveness of the proposed STF-EVD, comparative analyses with existing artifact removal methods were carried out across different performance metrics, using both ConvNet-DL and LDA-ML models, with results indicating that the proposed method achieved significantly better performance. It was also observed that the proposed method was able to preprocess the raw MI-EEG data effectively, resulting to high-quality signal that led to significant improvement in decoding accuracy for both the ConvNet-DL and LDA-ML models (Fig. 2.). Further analysis also indicated that the individual MI task can be adequately decoded with accuracies higher that 95% for both classification models when the proposed method is applied.

Despite the significant improvement recorded, the proposed method still needs some improvement as follows. Work is ongoing on making the proposed method fully automated by integrating an artifact detection algorithm that is able to self-identify artifact-dominated segments in the signal. Also more subjects will be recruited to further validate findings from this work. The outcome of this study could help inform the design of effective and robust control methods based on EEG pattern recognition for multiple degrees of freedom rehabilitation devices for patients with above-elbow amputations.

References

[1] Trujillo, P., Alfonso, M., Alessandro, S., et al. "Quantitative EEG for Predicting Upper Limb Motor Recovery in Chronic Stroke Robot-Assisted Rehabilitation," IEEE Transactions on Neural Systems and Rehabilitation Engineering, 25(7):1058-1067, 2017.

[2] Li, X. et al. "A motion-classification strategy based on sEMG-EEG signal combination for upper-limb amputees," Journal of NeuroEngineering & Rehabilitation, 14(1), pp.1-13, 2017.

[3] Feigin, V. L., et al. "Global burden of stroke and risk factors in 188 countries, during 1990–2013: a systematic analysis for the Global Burden of Disease Study 2013," The Lancet Neurology, 15(9), 913-924, 2016.

[4] Béjot, Y., Bailly, H., Durier, J. and Giroud, M., "Epidemiology of stroke in Europe and trends for the 21st century," La Presse Médicale, 45(12):e391-e398, 2016.

[5] Samuel, O. W., Asogbon, M. G., Geng, Y., Al-Timemy, A. H., Pirbhulal, S., Ji, N., ... & Li, G. "Intelligent EMG pattern recognition control method for upper-limb multifunctional prostheses: advances, current challenges, and future prospects," IEEE Access, 7, 10150-10165,2019.

[6] Gu, X., Cao, Z., Jolfaei, A., Xu, P., Wu, D., Jung, T. P., & Lin, C. T. "EEG-based brain-computer interfaces (BCIs): a survey of recent studies on signal sensing technologies and computational intelligence approaches and their applications," arXiv preprint arXiv:2001.11337, 2020.

[7] Padfield, N., Zabalza, J., Zhao, H., Masero, V., & Ren, J., "EEG-based brain-computer interfaces using motor- imagery: techniques and challenges". Sensors, 19(6), 1423, 2019.

[8] Jiang, X., Bian, G. B., & Tian, Z. "Removal of artifacts from EEG signals: a review. Sensors," 19(5), 987, 2019.

[9] Urigüen, J. A., & Garcia-Zapirain, B. "EEG artifact removal—state-of-the-art and guidelines," Journal of Neural Engineering, 12(3), 031001,2015.

[10] Anderer, P., Roberts, S., Schlögl, A., Gruber, G., Klösch, G., Herrmann, W., Rappelsberger, P., Filz, O., Barbanoj, M.J., Dorffner, G., et al. "Artifact processing in computerized analysis of sleep EEG—A review," Neuropsychobiology, 40, 150–157, 1999.

[11] Somers, B., Francart, T., & Bertrand, A., "A generic EEG artifact removal algorithm based on the multi-channel Wiener filter," Journal of Neural Engineering, 15(3), 036007, 2019.

[12] Wallstrom, G. L., Kass, R. E., Miller, A., Cohn, J. F., & Fox, N. A. "Automatic correction of ocular artifacts in the EEG: a comparison of regression-based and component-based methods," International Journal of Psychophysiology, 53(2), 105-119, 2004.

[13] Merinov, P., Belyaev, M., & Krivov, E., "The comparison of automatic artifact removal methods with robust classification strategies in terms of EEG classification accuracy." In 2015 International Conference on Biomedical Engineering and Computational Technologies (SIBIRCON), 221-224, 2015.

[14] Idowu, O. P., Ilesanmi, A. E., Li, X., Samuel, O.W., Fang, P., & Li, G. (2021). An Integrated Deep Learning Model for Motor Intention Recognition of Multi-Class EEG Signals in Upper Limb Amputees. Computer Methods and Programs in Biomedicine, 106121.

[15] Serizel, R., Moonen, M., Dijk, B.V., & Wouters, J. "Low-rank approximation based multichannel Wiener filter algorithms for noise reduction with application in cochlear implants," IEEE/ACM Transactions on Audio, Speech, and Language Processing, 22(4), 785–799, 2014.

[16] Samuel, O.W. et al., "Pattern recognition of electromyography signals based on novel time domain features for amputees' limb motion classification," Computers & Electrical Engineering, pp. 1-10, 2018.

[17] Geng, Y, et al. "A Robust Sparse Representation based Pattern Recognition Approach for Myoelectric Control," IEEE Access, 6, 38326 – 38335, 2019.

[18] Samuel, O.W et al. "Towards efficient decoding of multiple classes of motor imagery limb movements based on EEG spectral and time domain descriptors," Journal of medical systems, 41(12), 1-13, 2017.